

BiCo-Fusion: Bidirectional Complementary LiDAR-Camera Fusion for Semantic- and Spatial-Aware 3D Object Detection

Yang Song¹ and Lin Wang^{1,2,*}

Abstract—3D object detection is an important task that has been widely applied in autonomous driving. Recently, fusing multi-modal inputs, *i.e.*, LiDAR and camera data, to perform this task has become a new trend. Existing methods, however, either ignore the sparsity of Lidar features or fail to preserve the original spatial structure of LiDAR and the semantic density of camera features simultaneously due to the modality gap. To address issues, this letter proposes a novel bidirectional complementary Lidar-camera fusion framework, called BiCo-Fusion that can achieve robust semantic- and spatial-aware 3D object detection. The key insight is to mutually fuse the multi-modal features to enhance the semantics of LiDAR features and the spatial awareness of the camera features and adaptatively select features from both modalities to build a unified 3D representation. Specifically, we introduce Pre-Fusion consisting of a Voxel Enhancement Module (VEM) to enhance the semantics of voxel features from 2D camera features and Image Enhancement Module (IEM) to enhance the spatial characteristics of camera features from 3D voxel features. Both VEM and IEM are bidirectionally updated to effectively reduce the modality gap. We then introduce Unified Fusion to adaptively weight to select features from the enchanted Lidar and camera features to build a unified 3D representation. Extensive experiments demonstrate the superiority of our BiCo-Fusion against the prior arts. Project page: <https://t-ys.github.io/BiCo-Fusion/>.

Index Terms—Deep Learning for Visual Perception; Sensor Fusion; Object Detection, Segmentation and Categorization.

I. INTRODUCTION

3D object detection [1]–[3] is a critical and challenging task that aims to localize and classify objects in the 3D space, which has been widely applied in applications such as robotics and autonomous driving. Early works often resorted to one single sensor as inputs, such as LiDARs or RGB cameras. While approaches based on these two sensors have yielded significant results, yet they both have their own unsolvable problems. LiDAR-based methods [4]–[18] have difficulty detecting long-distance or small objects due to the sparsity of point cloud and the lack of semantics, while camera-based methods [19]–[26] perform even worse, struggling in localization due to the lack of accurate spatial and depth information, especially when the objects are occluded.

Recently, a new trend to handle these problems is to fuse two modalities, aiming to utilize more complementary information from both sparse point clouds and dense camera data. In the context of this trend, existing methods to deal with

the fusion of two heterogeneous modalities can be divided into two main categories: *i)* 2D-plane fusion (Fig. 1(a)) and *ii)* 3D-space fusion (Fig. 1(b)). 2D-plane fusion methods [2], [27]–[32] perform LiDAR-camera fusion by projecting point clouds to the image plane and retrieving the nearby 2D features, which are used to decorate the 3D representations for compensating the semantic capabilities. However, such a projection ignores the sparsity of LiDAR data, and inevitably wastes semantically rich 2D features [33].

3D-space fusion methods, on the other hand, unify two modalities in the same space [1], [3], [34], either in the voxel space [3] or in bird’s eye view (BEV) space [1]. During the fusion in a unified space, the sparsity of geometry is well resolved by the dense features from the camera, making the performance significantly stronger than that of 2D-plane fusion. Despite the impressive improvements, the modality gap makes it fail to preserve the original strengths of these two modalities simultaneously. Specifically, although it is expected to fuse the strong representations from two modalities, *i.e.*, the strong spatial capability of LiDAR and the dominant semantic density of the camera. It can not be neglected that these two modalities also have their drawbacks (*i.e.*, LiDAR lacks semantics and camera struggles in spatial perception), which are also fused when building a unified 3D representation. Such a ‘*negative effect*’ renders the fused features often imperfect. In other words, it weakens the impact of the strong aspects of the original modality, leading to a substantial loss of modality-specific strengths.

In this letter, we propose **BiCo-Fusion**, a novel multi-modal 3D object detection framework to tackle the above problems. BiCo-Fusion employs a bidirectional complementary strategy to mutually fuse the multi-modal features to enhance the semantics of LiDAR features and the spatial awareness of the camera features and adaptatively select features from both modalities to build a unified 3D representation, as shown in Fig. 1(c). This subtly ensures semantic and spatial awareness and reduces the modality gap, thereby facilitating a smoother and more efficient fusion. Firstly, the extracted features from LiDAR and the camera are input into the initial stage of fusion, referred to as *Pre-Fusion* (Sec. III-B). Here, two modules play crucial roles: the Voxel Enhancement Module (VEM) projects non-empty voxels onto the image plane and extracts the surrounding camera features to enhance their semantics, which is optimized based on our distance-prior weighting scheme. The Image Enhancement Module (IEM) fuses the real depth from the LiDAR with camera features to enhance their spatial awareness. Through Pre-Fusion, the drawbacks of both modalities undergo specific

*Corresponding author

¹Yang Song is with the AI Thrust, The Hong Kong University of Science and Technology (Guangzhou), Guangdong 511458, China. ysong196@connect.hkust-gz.edu.cn

^{1,2}Lin Wang is with A/CMA Thrust, HKUST(GZ) and Dept. of CSE, HKUST, Hong Kong SAR, China, Email: linwang@ust.hk

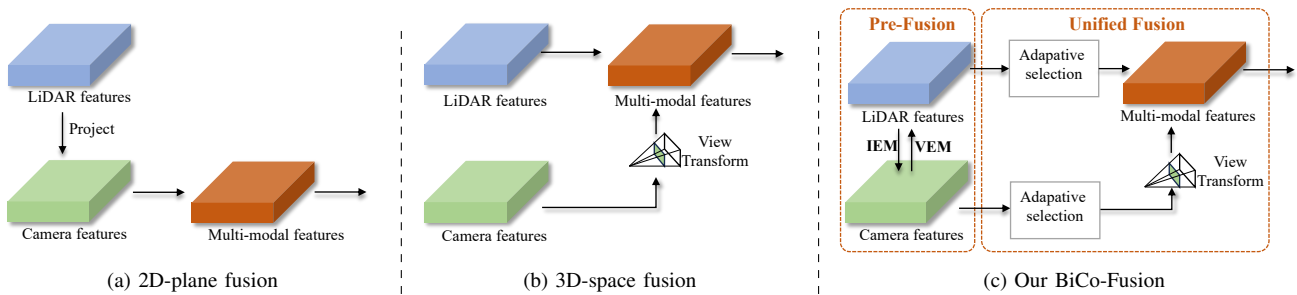


Fig. 1. **Comparison of our framework with previous LiDAR-camera fusion methods.** (a) 2D-plane fusion projects point clouds to the image plane and retrieves the corresponding 2D features which are used to augment original points. (b) 3D-space fusion firstly estimates the depth of images and then lifts them by view transform to a unified space, where the two modalities are fused. (c) Our BiCo-Fusion proposes a bidirectional complementary fusion to reduce the modality gap and achieve a smoother process. In the initial Pre-Fusion stage, we introduce VEM and IEM to apply specific enhancements to each modality which provide semantics for LiDAR and spatial capability for camera, respectively. During Unified Fusion, the enhanced features are unified in a 3D space by view transformation for further adaptive-weighted-based fusion.

enhancements, avoiding the negative effect, thus reducing the modality gap. Next, we lift the enhanced camera features to a unified voxel space by view transformation [19], which is fused with the enhanced LiDAR voxel features. We then introduce an adaptive weighting scheme to perform *Unified Fusion* to dynamically select the 3D features that possess both spatial-semantic awareness (Sec. III-C). Overall, these components work seamlessly to guarantee a more robust 3D representation for the detection.

Extensive experiments on the nuScenes [35] benchmark demonstrate that our BiCo-Fusion approach achieves state-of-the-art (SoTA) performance, with 72.4% mAP and 74.5% NDS on the test set. In summary, our contributions are three-fold: **(I)** We propose a novel multi-modal fusion framework for 3D object detection task, employing bidirectional complementary LiDAR-camera fusion to preserve the spatial structure from LiDAR and the semantics from camera, which reduces the modality gap, allowing for a more comprehensive 3D representation; **(II)** We propose Pre-Fusion with VEM for enhancing the semantics of voxels and IEM for enhancing the spatial awareness of camera data, and Unified Fusion for adaptively unifying representations in the 3D voxel space; **(III)** We achieve the SOTA 3D detection performance on the challenging nuScenes dataset.

II. RELATED WORK

LiDAR-based 3D Object Detection. LiDAR point clouds are inherently suitable for 3D object detection, in that they can provide accurate 3D spatial information. However, the point cloud data is sparse, disordered, and redundant, which results in point cloud data that cannot be directly fed into a CNN network for feature extraction. PointNet [36] is the first backbone capable of extracting point cloud features, After that, a great deal of subsequent works, *e.g.*, [8], [16], [17] have been proposed. Later, to obtain more regular point cloud data, researchers choose to rasterize point cloud data into discrete grid representation, such as voxels [4], [13], [15] and pillars [5]. These approaches enable direct feature extraction with convolutional networks. However, they cannot break the limitation of using a single modality and are prone to false detections due to missing semantics in special cases, such as

small and distant objects. In contrast, our method uses both LiDAR and camera data and mutually fuses the multi-modal features to enhance the semantics of LiDAR features and the spatial awareness of the camera features.

LiDAR-Camera Fusion-based 3D Object Detection. This has become a new trend, dedicated to maximizing the use of both worlds. Early works typically use a projection strategy to retrieve image features for decorating point clouds. PointPainting [27] is a pioneering work to enhance semantic capabilities by projecting semantic segmentation labels of images into the point cloud space. While MV3D [28] projects 3D proposals into 2D plane for connecting two modalities. TransFusion [2] uses the attention mechanism to selectively fuse relevant image features to the point cloud. Thanks to lift-splat-shoot (LSS) [19], recent research efforts are mostly based on it to transform camera features into the same unified space with LiDAR. BEVFusion [1] provides a new pipeline that unifies the two modalities in birds' eye view (BEV) space. While UVTR [3] uses the two modalities by unifying them in voxel space to avoid the dislocation effect of height collapse. However, these methods fail to preserve the original spatial structure of LiDAR and the semantic density of camera features simultaneously due to the modality gap. *By contrast, our BiCo-Fusion proposes a bidirectional complementary strategy to mutually fuse the multi-modal features to enhance the semantics of LiDAR features and the spatial awareness of the camera features, which are adaptively weighted to build a unified 3D representation.*

III. METHODOLOGY

A. Framework Overview

As shown in Fig. 2, given the raw LiDAR and RGB camera data as inputs, we first extract features from specific encoders. Following BEVFusion [1], we use VoxelNet [4] as the LiDAR encoder and Swin Transformer [37] as the camera encoder, respectively.

Then, the extracted LiDAR voxel features F_L and camera features F_C are interacted with and fused using our designed method. Our multi-modal fusion space contains two fusions, in the Pre-Fusion phase, our Voxel Enhancement Module (VEM) and Image Enhancement Module (IEM) modules

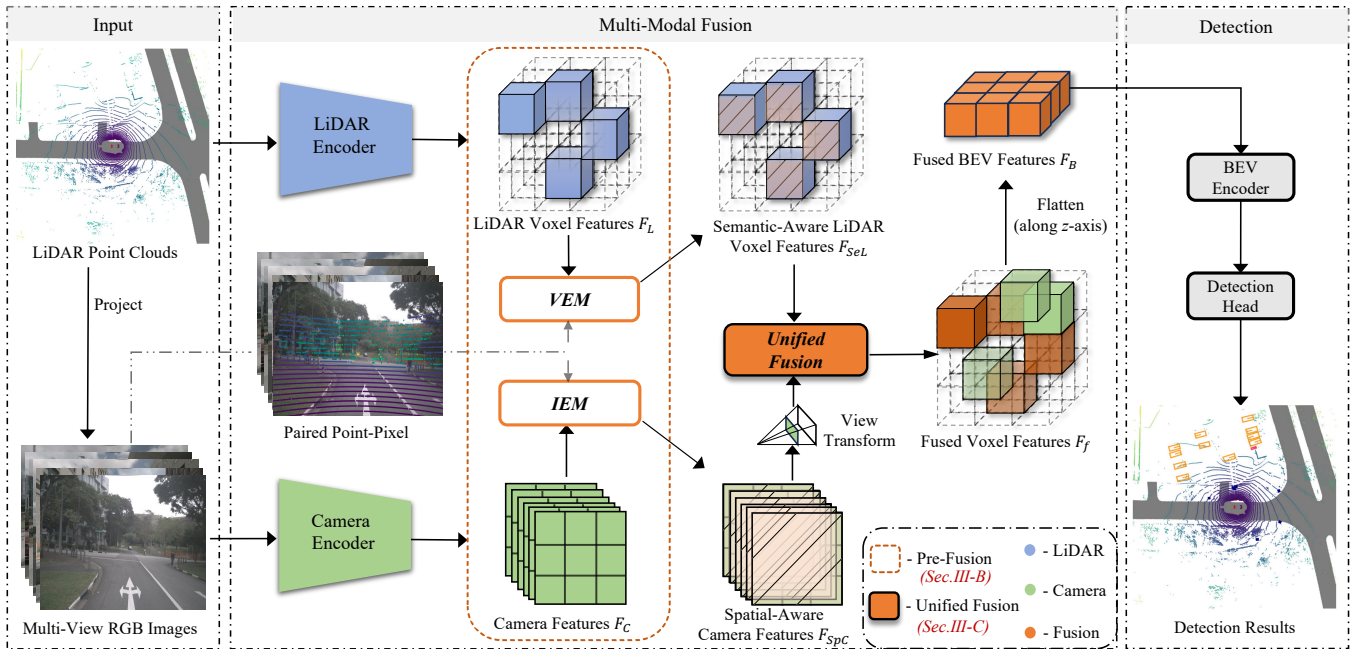


Fig. 2. **Overview of our BiCo-Fusion framework.** BiCo-Fusion first extracts features from LiDAR and camera data using modality-specific encoders. In Pre-Fusion, the LiDAR voxel features are enhanced with the camera semantics by our VEM, and the camera features are enhanced to be spatial-aware with the IEM. These enhanced features are then fused in an adaptive way during the Unified Fusion stage. Finally, the fused features are flattened to get the BEV features, which are fed to the head for final detection.

perform specific bidirectional complementary enhancement for both modalities to improve the semantic capability of voxels and the spatial capability of images, which effectively avoids the negative effects caused by the weak representations, and also prepares more comprehensive features for the next step. Afterward, in the Unified Fusion phase (U-Fusion), the enhanced spatial-aware camera features F_{SpC} then be lifted into the 3D voxel space by view transformation [1], [3], [19], which are further fused with the semantic-aware LiDAR voxel features F_{SeL} in an adaptive way.

Finally, following the workflow of the voxel-based approaches [1], [4], [6], we collapse the height of the fused voxel features F_f in order to transform them into the BEV space, then the BEV features F_B go through the convolutional-based BEV encoder and the detection head for obtaining the final 3D detection results. Following UVTR [3], the Hungarian algorithm is applied to match the predictions and the ground truth during training. Meanwhile, Focal loss [38] and $L1$ loss are used for the classification and 3D bounding box regression, respectively.

B. Pre-Fusion

The Pre-Fusion consists of two key modules: the VEM and the IEM. These two modules work in a bidirectional complementary manner to enhance the semantics of voxels and the spatial characteristics of images. It mitigates the weak representations of LiDAR and camera. Meanwhile, the strong representations of them are preserved, allowing for a more comprehensive 3D representation.

1) *Voxel Enhancement Module*: Despite having strong spatial localization capabilities, the LiDAR voxel features F_L

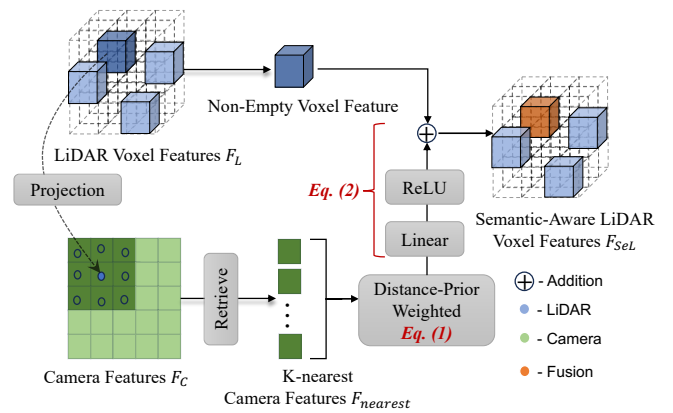


Fig. 3. **Voxel Enhancement Module (VEM).** VEM first projects voxel to the image plane to retrieve the K nearest camera features. Then, the camera features are weighted in a distance-prior way, which then be inputted to a Linear layer for achieving a learnable process. Finally, the resulted camera features are fused with the original LiDAR voxel features by addition.

obtained from the LiDAR branch lack important semantic information. This drawback can propagate through the Unified Fusion process. To overcome this issue and provide more comprehensive features for the Unified Fusion, we design the VEM, as shown in Fig. 3.

In the VEM, the center point of every non-empty voxel is first projected onto image coordinates using the intrinsic and extrinsic parameters. To mitigate incorrect alignments, we then retrieve the K nearest camera features $F_{nearest} \in \mathbb{R}^{K \times C_{2D}}$ around the projection point. During fusion, the contribution of these camera features should be different, so we designed a distance-prior weighting scheme. Specif-

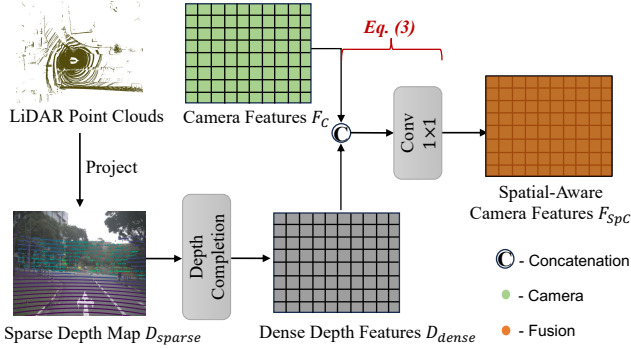


Fig. 4. **Image Enhancement Module (IEM)**. It first projects raw LiDAR points to the image coordinates. Then, we use depth completion to generate a dense depth feature map, whose size is the same as the camera features. Finally, the dense depth feature map is concatenated with the camera features, followed by a convolution layer to reduce the feature dimension.

ically, for the K camera features, we first calculate the reciprocals of the distances to the projection point, denoted as $L_{nearest} \in \mathbb{R}^{1 \times K}$, which is formed as the weights for $F_{nearest}$. Then, we obtain the distance-prior weighted camera features $F_{weighted} \in \mathbb{R}^{1 \times C_{2D}}$ as:

$$F_{weighted} = \text{Softmax}(L_{nearest}) \times F_{nearest}, \quad (1)$$

where the Softmax function is used to calculate the weights of different camera features.

Finally, we use a Linear layer and an activation function followed by addition to achieve a learnable fusion process, resulting in the semantic-aware voxel features, denoted as F_{SeL} . The whole process can be defined by:

$$F_{SeL} = \text{ReLU}(\text{Linear}(F_{weighted})) + F_L. \quad (2)$$

2) *Image Enhancement Module*: Camera features lack the perception ability of 3D spatial information, which is crucial for 3D object detection tasks. To enhance them from this view, we propose IEM, as shown in Fig. 4. We first project the point cloud onto the image plane to obtain a sparse depth map D_{sparse} . Inspired by [39], we then use depth completion [40] followed by feature extraction to obtain a dense depth feature map $D_{dense} \in \mathbb{R}^{H \times W \times C_{depth}}$. Finally, we concatenate the dense depth feature map with the camera features $F_C \in \mathbb{R}^{H \times W \times C_{2D}}$ and use a convolutional layer to fuse them, getting the spatial-aware camera features F_{SpC} :

$$F_{SpC} = \text{Conv}(\text{Concat}(F_C, D_{dense})). \quad (3)$$

Due to the geometric capability of the spatially-aware camera features, lifting them into 3D space ensures a more accurate process, providing a solid foundation for the subsequent Unified Fusion.

C. Unified Fusion

After obtaining the semantic-aware LiDAR voxel features and spatial-aware camera features, which have undergone specific bidirectional complementarity during Pre-Fusion, we further fuse them in the U-Fusion stage to ensure the

integrity of strong representations, for both semantic and spatial levels.

Previous work [1], [34] unifies the two modalities in the BEV space by view transform. While this improved efficiency, it has an inherent limitation that prevents the fine-grained fusion which is vital for better performance. Therefore, after elevating the camera features to the voxel representation, we preserve its state, obtaining \hat{F}_{SpC} .

Given the enhanced features from both LiDAR ($F_{SeL} \in \mathbb{R}^{X \times Y \times Z \times C_{3D}}$) and Camera ($\hat{F}_{SpC} \in \mathbb{R}^{X \times Y \times Z \times C_{2D}}$) with same spatial dimensions, a straightforward idea is to directly concatenate them. Inspired by [41], to dynamically select features from both modalities, we have used an adaptive weighting method to perform Unified Fusion as:

$$\alpha = \mathcal{C}_{3D}(\text{Concat}(\mathcal{C}_{3D}(F_{SeL}), \mathcal{C}_{3D}(\hat{F}_{SpC}))), \quad (4)$$

$$F_f = \sigma(\alpha) \cdot F_{SeL} + (1 - \sigma(\alpha)) \cdot \hat{F}_{SpC}, \quad (5)$$

where \mathcal{C}_{3D} refers to 3D convolution, σ denotes *Sigmoid* activation, and F_f is the fused unified features in voxel space.

IV. EXPERIMENTS

A. Experimental Setup

Dataset. Following previous works [1], [2], we evaluate the 3D object detection performance of our BiCo-Fusion on the nuScenes benchmark [35]. The nuScenes dataset is a large-scale autonomous driving benchmark including 10,000 driving scenarios in total (700, 150, and 150 scenes for training, validation, and testing, respectively). To evaluate 3D object detection, there are two main metrics: mean Average Precision (mAP) and nuScenes detection scores (NDS). The mAP is calculated from the mean of the average precision across ten classes under distance thresholds of 0.5m, 1m, 2m, and 4m. NDS is a comprehensive metric that integrates mAP with five True Positive (TP) metrics: mATE, mASE, mAOE, mAVE, and mAAE, which together ensure a robust evaluation of object translation, scale, orientation, velocity, and attributes.

Implementation Details. Our implementation is based on the MMDetection3D framework [48]. We use Swin-T [37] as our image backbone and VoxelNet [4] as our LiDAR backbone. We set the image size to 384×1056 and voxelize the LiDAR point cloud with 0.075m, and the point cloud covers [-54m, 54m] along the X and Y axes, [-5m, 3m] along the Z axis, respectively. Our model is trained with a batch size of 16. Following [2], our training consists of two stages: (1) We first train the LiDAR-only baseline for 20 epochs. (2) We then finetune the proposed LiDAR-camera fusion framework for another 6 epochs. We follow CBGS [49] to perform class-balanced sampling and employ the AdamW optimizer [50] with one cycle learning rate policy [51], with max learning rate $1e^{-3}$, weight decay 0.01.

B. Main Results

We compare our BiCo-Fusion with leading methods on the nuScenes test set, as shown in Tab. I. It demonstrates

TABLE I
PERFORMANCE COMPARISON OF DIFFERENT METHODS. ‘L’ AND ‘C’ DENOTE THE LiDAR AND THE CAMERA. ‘C.V.’, ‘MOTOR.’, ‘PED.’, AND ‘T.C.’ REFER TO THE CONSTRUCTION VEHICLE, MOTORCYCLE, PEDESTRIAN, AND TRAFFIC CONE, RESPECTIVELY. ‘†’ DENOTES THE MODEL WITH TEST-TIME AUGMENTATION AND MODEL ENSEMBLE TECHNIQUES.

Method	Modality	mAP	NDS	Car	Truck	C.V.	Bus	Trailer	Barrier	Motor.	Bike	Ped.	T.C.
PointPillars [5]	L	40.1	55.0	76.0	31.0	11.3	32.1	36.6	56.4	34.2	14.0	64.0	45.6
CenterPoint [6]	L	60.3	67.3	85.2	53.5	20.0	63.6	56.0	71.1	59.5	30.7	84.6	78.4
TransFusion-L [2]	L	65.5	70.2	86.2	56.7	28.2	66.3	58.8	78.2	68.3	44.2	86.1	82.0
FocalFormer3D [42]	L	68.7	72.6	87.2	57.1	34.4	69.6	64.9	77.8	76.2	49.6	88.2	82.3
Pointpainting [27]	L+C	46.4	58.1	77.9	35.8	15.8	36.2	37.3	60.2	41.5	24.1	73.3	62.4
MVP [43]	L+C	66.4	70.5	86.8	58.5	26.1	67.4	57.3	74.8	70.0	49.3	89.1	85.0
PointAugmenting [31]	L+C	66.8	71.0	87.5	57.3	28.0	65.2	60.7	72.6	74.3	50.9	87.9	83.6
UVTR [3]	L+C	67.1	71.1	87.5	56.0	33.8	67.5	59.5	73.0	73.4	54.8	86.3	79.6
AutoAlignV2 [44]	L+C	68.4	72.4	87.0	59.0	33.1	69.3	59.3	-	72.9	52.1	87.6	-
TransFusion-LC [2]	L+C	68.9	71.7	87.1	60.0	33.1	68.3	60.8	78.1	73.6	52.9	88.4	86.7
BEVFusion [34]	L+C	69.2	71.8	88.1	60.9	34.4	69.3	62.1	78.2	72.2	52.2	89.2	85.2
BEVFusion [1]	L+C	70.2	72.9	88.6	60.1	39.3	69.8	63.8	80.0	74.1	51.0	89.2	86.5
DeepInteraction [39]	L+C	70.8	73.4	87.9	60.2	37.5	70.8	63.8	80.4	75.4	54.5	90.3	87.0
UniTR [45]	L+C	70.9	74.5	87.9	60.2	39.2	72.2	65.1	76.8	75.8	52.2	89.4	89.7
MSMDFusion [33]	L+C	71.5	74.0	88.4	61.0	35.2	71.4	64.2	80.7	76.9	58.3	90.6	88.1
FocalFormer3D [42]	L+C	71.6	73.9	88.5	61.4	35.9	71.7	66.4	79.3	80.3	57.1	89.7	85.3
SparseFusion [46]	L+C	72.0	73.8	88.0	60.2	38.7	72.0	64.9	79.2	78.5	59.8	90.9	87.9
CMT [47]	L+C	72.0	74.1	88.0	63.3	37.3	75.4	65.4	78.2	79.1	60.6	87.9	84.7
BiCo-Fusion (Ours)	L+C	72.4	74.5	88.1	61.9	38.2	73.3	65.7	80.4	78.9	59.8	89.7	88.3
BiCo-Fusion [†] (Ours)	L+C	76.1	77.1	89.6	67.4	44.1	76.4	66.8	83.5	82.6	65.9	93.6	90.8

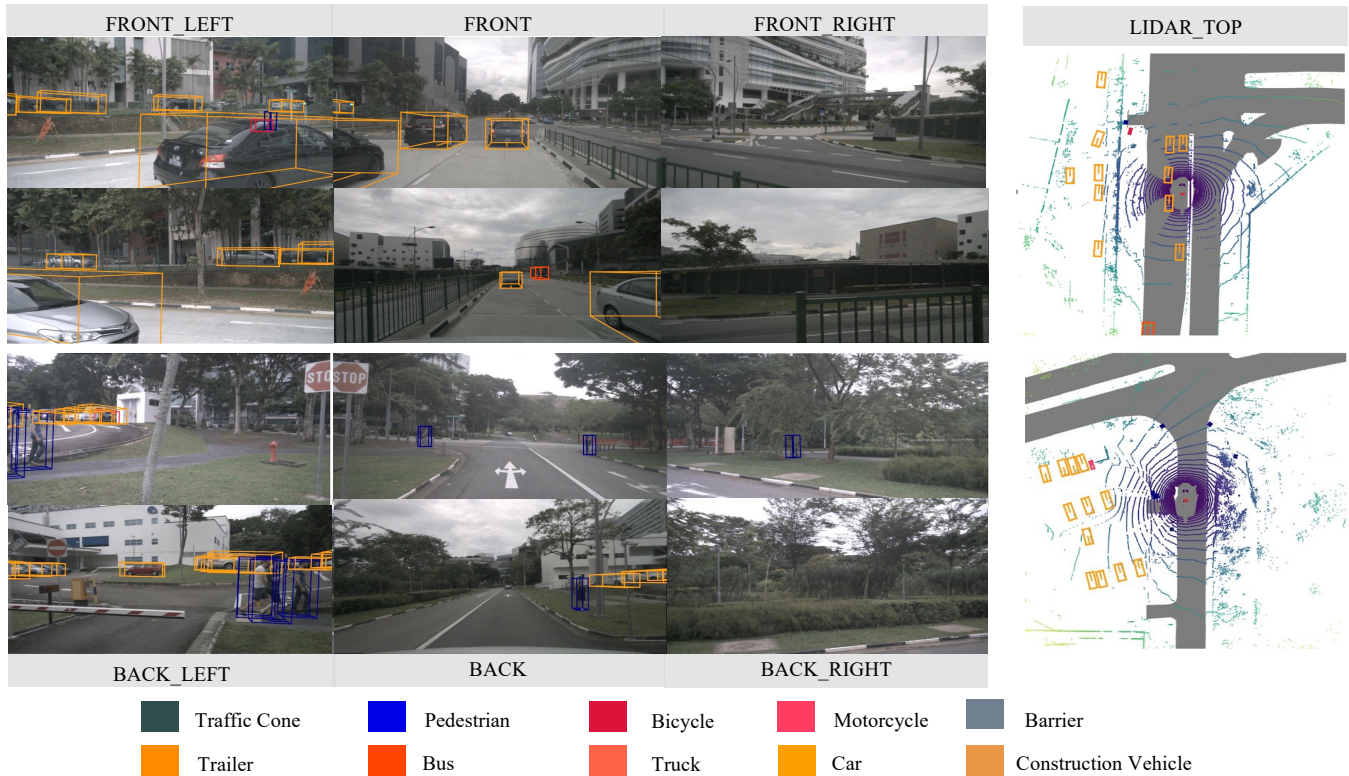


Fig. 5. Qualitative results of BiCo-Fusion on nuScenes validation set.

that BiCo-Fusion significantly improves the LiDAR-only baseline, TransFusion-L [2], by 6.9% mAP and 4.3% NDS, due to the additional fusion of multi-modalities. More importantly, BiCo-Fusion achieves superior performance compared to prior works, with 72.4% mAP and 74.5% NDS. By combining test-time augmentation and model ensemble

techniques, BiCo-Fusion[†] further achieves a state-of-the-art (SOTA) performance. In Fig. 5, we also present some qualitative results on the nuScenes validation set, which shows that our method can detect challenging cases even when the small objects are occluded or many objects are tightly packed together.

TABLE II

ABLATION STUDIES FOR OUR PROPOSED COMPONENTS ON THE nuSCENES VALIDATION SET.

	Baseline	VEM	IEM	U-Fusion	mAP	NDS
(1)	✓				64.6	69.3
(2)	✓	✓			66.5	70.3
(3)	✓	✓		✓	70.0	72.5
(4)	✓	✓	✓	✓	70.5	72.9

TABLE III

PARAMETER SELECTION IN VOXEL ENHANCEMENT MODULE.

Number of camera surroundings (K)	mAP	NDS
1	69.2	71.9
3	69.8	72.4
6	70.3	72.7
9	70.5	72.9
10	70.4	72.9

C. Ablation Studies

1) *Component-wise Ablation*: As shown in Tab. II, we conduct ablation studies on our proposed modules on the nuScenes validation set. In Tab. II (1), we reimplement TransFusion-L [2] as our LiDAR-only baseline. According to Tab. II (2), after combing VEM, we improve mAP by 1.9% and NDS by 1%, which indicates the effectiveness of enhancing the semantic capability of voxel features. Furthermore, incorporating the Unified Fusion (U-Fusion) leads to additional improvement by 3.5% mAP and 2.2% NDS (Tab. II (3)). It should be emphasized that there are two main reasons why the combination with Unified Fusion contributes to such a big improvement: a) The Voxel Enhancement Module in Pre-Fusion reduces the modality gap, setting the stage for the second step of fusion. b) The fusion in a unified voxel space fills in many non-empty voxels, compensating for the geometric sparsity of the LiDAR modality.

Finally, with all these components combined (Tab. II (4)), the final mAP and NDS achieve significant enhancement to 70.5% and 72.9%, respectively, which demonstrates that enhancing the spatial capability of camera features can further decrease the negative effect and help to guarantee the strong representations can be preserved.

2) *Discussion on Voxel Enhancement Module*: We analyze the selection of the number of surrounding camera features per voxel (K) in the voxel enhancement module. As shown in Tab. III, when K increases from 1 to 9, the mAP and NDS gradually rise. And when K is increased to 10, there is no change in NDS, but the mAP decreases, so we select $K = 9$ for the framework.

Tab. IV demonstrates the effectiveness of our distance-prior weighting scheme in the voxel enhancement module, which improves the mAP and NDS by 0.8% and 0.6%, respectively.

3) *Discussion on Unified Fusion*: In Unified Fusion (U-Fusion), we employ an adaptive weighted fusion method, which dynamically selects features from both modalities for fusing in unified voxel space. We ablate it in Tab. V, which indicates that our scheme improves performance compared

TABLE IV

EFFECT OF DISTANCE-PRIOR WEIGHTING SCHEME IN VEM.

Weighting scheme in VEM	mAP	NDS
w/o distance-prior	69.7	72.3
w/ distance-prior	70.5	72.9

TABLE V

EFFECT OF ADAPTIVE WEIGHTING IN U-FUSION

Weighting scheme in U-Fusion	mAP	NDS
w/o adaptive weighting	69.4	72.2
w/ adaptive weighting	70.5	72.9

TABLE VI

ABLATION STUDIES FOR DIFFERENT CHOICES IN FRAMEWORK

	Different Choices	mAP	NDS
(a) Image backbone	ResNet-50	69.4	72.1
	ResNet-101	70.1	72.6
	Swin-T	70.5	72.9
(b) Voxel size	0.075	70.5	72.9
	0.1	70.0	72.5
(c) Image size	256 x 704	69.9	72.5
	384 x 1056	70.5	72.9

with simple concatenation, by 1.1% mAP and 0.7% NDS.

4) *Ablation on Different Choices in Framework*: We further construct ablation studies on different choices in our BiCo-Fusion framework. As shown in Tab. VI (a), our framework can benefit from more powerful image backbones. Swin-T [37] achieves the best performance, with improving mAP by 1.1%, compared with ResNet [52]. Tab. VI (b) demonstrates that a smaller voxel size can bring a small-scale improvement, with about 0.5% for both mAP and NDS. Same as voxel size, using a larger image resolution (*e.g.*, 384×1056) also leads to a slight performance improvement, as shown in Tab. VI (c).

V. CONCLUSIONS

This letter presented BiCo-Fusion, a novel framework that employs a bidirectional complementary LiDAR-camera fusion strategy to preserve the spatial structure of LiDAR and the semantic features of the camera, ensuring a reduction of the modality gap for robust 3D object detection. We introduced the Pre-Fusion and Unified Fusion (U-Fusion) to enhance the semantics of LiDAR voxel features and spatial capability of camera features and adaptively fuse the enhanced features from both modalities in a unified voxel space. Extensive experiments demonstrated the effectiveness of these components and our proposed framework.

Limitations and Future Work. At present, BiCo-Fusion uses a simple projection and retrieval mechanism in Pre-Fusion, which relies on alignments on the nuScenes dataset. We believe that this can be better optimized by introducing a softer attention mechanism to avoid some calibration inaccuracies. Besides, a supervised depth estimation [23] is able to further enhance the spatial structure of the final 3D representation from the camera branch, which ensures better performance. We leave these limitations as future work.

REFERENCES

- [1] Z. Liu, H. Tang, M. Amini, X. Yang, H. Mao, O. Daniela, R. Mit, H. Song, and M. Mit, "Bevfusion: Multi-task multi-sensor fusion with unified bird's-eye view representation," in *ICRA*, 2023.
- [2] X. Bai, Z. Hu, X. Zhu, Q. Huang, Y. Chen, H. Fu, and C.-L. Tai, "Transfusion: Robust lidar-camera fusion for 3d object detection with transformers," in *CVPR*, 2022.
- [3] Y. Li, Y. Chen, X. Qi, Z. Li, J. Sun, and J. Jia, "Unifying voxel-based representation with transformer for 3d object detection," in *NeurIPS*, 2022.
- [4] Y. Zhou and O. Tuzel, "Voxelnet: End-to-end learning for point cloud based 3d object detection," in *2018 IEEE/CVF Conference on Computer Vision and Pattern Recognition*, Jun 2018.
- [5] A. Lang, S. Vora, H. Caesar, L. Zhou, J. Yang, and O. Beijbom, "Pointpillars: Fast encoders for object detection from point clouds," in *CVPR*, 2019.
- [6] T. Yin, X. Zhou, and P. Krahenbuhl, "Center-based 3d object detection and tracking," in *CVPR*, 2021.
- [7] Y. Chen, Y. Li, X. Zhang, J. Sun, and J. Jia, "Focal sparse convolutional networks for 3d object detection," Apr 2022.
- [8] Y. Chen, S. Liu, X. Shen, and J. Jia, "Fast point r-cnn," in *2019 IEEE/CVF International Conference on Computer Vision (ICCV)*, Oct 2019. [Online]. Available: <http://dx.doi.org/10.1109/iccv.2019.00987>
- [9] C. He, R. Li, S. Li, and L. Zhang, "Voxel set transformer: A set-to-set approach to 3d object detection from point clouds."
- [10] Z. Yang, Y. Sun, S. Liu, and J. Jia, "3dssd: Point-based 3d single stage object detector," in *2020 IEEE/CVF Conference on Computer Vision and Pattern Recognition (CVPR)*, Jun 2020.
- [11] T. Feng, W. Wang, F. Ma, and Y. Yang, "Lsk3dnet: Towards effective and efficient 3d perception with large sparse kernels," in *CVPR*, 2024.
- [12] Y. Wang, A. Fathi, A. Kundu, D. A. Ross, C. Pantofaru, T. Funkhouser, and J. Solomon, *Pillar-based Object Detection for Autonomous Driving*, Jan 2020, p. 18–34.
- [13] J. Deng, S. Shi, P. Li, W. Zhou, Y. Zhang, and H. Li, "Voxel r-cnn: Towards high performance voxel-based 3d object detection," *Proceedings of the AAAI Conference on Artificial Intelligence*, p. 1201–1209, Sep 2022.
- [14] Z. Yang, Y. Sun, S. Liu, X. Shen, and J. Jia, "Std: Sparse-to-dense 3d object detector for point cloud," in *2019 IEEE/CVF International Conference on Computer Vision (ICCV)*, Oct 2019.
- [15] Y. Yan, Y. Mao, and B. Li, "Second: Sparsely embedded convolutional detection," *Sensors*, p. 3337, Oct 2018.
- [16] W. Shi and R. Rajkumar, "Point-gnn: Graph neural network for 3d object detection in a point cloud," in *2020 IEEE/CVF Conference on Computer Vision and Pattern Recognition (CVPR)*, Jun 2020.
- [17] S. Shi, X. Wang, and H. Li, "Pointcnn: 3d object proposal generation and detection from point cloud," in *2019 IEEE/CVF Conference on Computer Vision and Pattern Recognition (CVPR)*, Jun 2019.
- [18] C. R. Qi, W. Liu, C. Wu, H. Su, and L. J. Guibas, "Frustum pointnets for 3d object detection from rgb-d data," in *2018 IEEE/CVF Conference on Computer Vision and Pattern Recognition*, Jun 2018.
- [19] J. Philion and S. Fidler, *Lift, Splat, Shoot: Encoding Images from Arbitrary Camera Rigs by Implicitly Unprojecting to 3D*, Jan 2020, p. 194–210.
- [20] G. Brazil and X. Liu, "M3d-rpn: Monocular 3d region proposal network for object detection," in *2019 IEEE/CVF International Conference on Computer Vision (ICCV)*, Oct 2019.
- [21] T. Wang, X. Zhu, J. Pang, and D. Lin, "Fcos3d: Fully convolutional one-stage monocular 3d object detection," in *2021 IEEE/CVF International Conference on Computer Vision Workshops (ICCVW)*, Oct 2021.
- [22] J. Huang, G. Huang, Z. Zhu, and D. Du, "Bevdet: High-performance multi-camera 3d object detection in bird-eye-view."
- [23] Y. Li, Z. Ge, G. Yu, J. Yang, Z. Wang, Y. Shi, J. Sun, Z. Li, and M. Face++, "Bevdepth: Acquisition of reliable depth for multi-view 3d object detection."
- [24] Z. Li, W. Wang, H. Li, E. Xie, C. Sima, T. Lu, Y. Qiao, and J. Dai, *BEVFormer: Learning Bird's-Eye-View Representation from Multi-Camera Images via Spatiotemporal Transformers*, Jan 2022, p. 1–18.
- [25] Y. Wang, V. Guizilini, T. Zhang, Y. Wang, H. Zhao, and J. Solomon, "Detr3d: 3d object detection from multi-view images via 3d-to-2d queries," *Cornell University - arXiv, Cornell University - arXiv*, Oct 2021.
- [26] Y. Liu, T. Wang, X. Zhang, and J. Sun, "Petr: Position embedding transformation for multi-view 3d object detection."
- [27] S. Vora, A. H. Lang, B. Helou, and O. Beijbom, "Pointpainting: Sequential fusion for 3d object detection," in *CVPR*, 2020.
- [28] X. Chen, H. Ma, J. Wan, B. Li, and T. Xia, "Multi-view 3d object detection network for autonomous driving," in *CVPR*, 2017.
- [29] T. Huang, Z. Liu, X. Chen, and X. Bai, "Epnets: Enhancing point features with image semantics for 3d object detection," July 2020.
- [30] Y. Li, A. Yu, T. Meng, B. Caine, J. Ngiam, D. Peng, J. Shen, B. Wu, Y. Lu, D. Zhou, Q. Le, A. Yuille, and M. Tan, "Deepfusion: Lidar-camera deep fusion for multi-modal 3d object detection," in *CVPR*, 2022.
- [31] C. Wang, C. Ma, M. Zhu, and X. Yang, "Pointaugmenting: Cross-modal augmentation for 3d object detection," in *CVPR*, 2021.
- [32] M. Liang, B. Yang, Y. Chen, R. Hu, and R. Urtasun, "Multi-task multi-sensor fusion for 3d object detection," in *CVPR*, 2019.
- [33] Y. Jiao, Z. Jie, S. Chen, J. Chen, X. Wei, L. Ma, and Y.-G. Jiang, "Msmdfusion: Fusing lidar and camera at multiple scales with multi-depth seeds for 3d object detection," in *CVPR*, 2023.
- [34] T. Liang, H. Xie, K. Yu, Z. Xia, Z. Lin, Y. Wang, B. Wang, and Z. Tang, "Bevfusion: A simple and robust lidar-camera fusion framework," in *NeurIPS*, 2022.
- [35] H. Caesar, V. Bankiti, A. H. Lang, S. Vora, V. E. Liong, Q. Xu, A. Krishnan, Y. Pan, G. Baldan, and O. Beijbom, "nusscenes: A multimodal dataset for autonomous driving," in *2020 IEEE/CVF Conference on Computer Vision and Pattern Recognition (CVPR)*, Jun 2020.
- [36] R. Q. Charles, H. Su, M. Kaichun, and L. J. Guibas, "Pointnet: Deep learning on point sets for 3d classification and segmentation," in *2017 IEEE Conference on Computer Vision and Pattern Recognition (CVPR)*, Jul 2017.
- [37] Z. Liu, Y. Lin, Y. Cao, H. Hu, Y. Wei, Z. Zhang, S. Lin, and B. Guo, "Swin transformer: Hierarchical vision transformer using shifted windows," in *2021 IEEE/CVF International Conference on Computer Vision (ICCV)*, Oct 2021.
- [38] T.-Y. Lin, P. Goyal, R. Girshick, K. He, and P. Dollár, "Focal loss for dense object detection," in *2017 IEEE International Conference on Computer Vision (ICCV)*, 2017, pp. 2999–3007.
- [39] Z. Yang, J. Chen, Z. Miao, W. Li, X. Zhu, and L. Zhang, "Deepinteraction: 3d object detection via modality interaction," in *NeurIPS*, 2022.
- [40] J. Ku, A. Harakeh, and S. L. Waslander, "In defense of classical image processing: Fast depth completion on the cpu," in *2018 15th Conference on Computer and Robot Vision (CRV)*, May 2018.
- [41] X. Wang, Z. Zhu, W. Xu, Y. Zhang, Y. Wei, X. Chi, Y. Ye, D. Du, J. Lu, and X. Wang, "Openoccupancy: A large scale benchmark for surrounding semantic occupancy perception," Mar 2023.
- [42] Y. Chen, Z. Yu, Y. Chen, S. Lan, A. Anandkumar, J. Jia, and J. M. Alvarez, "Focalformer3d: Focusing on hard instance for 3d object detection," in *ICCV*, 2023.
- [43] T. Yin, X. Zhou, and P. Krähenbühl, "Multimodal virtual point 3d detection," in *NeurIPS*, 2021.
- [44] Z. Chen, Z. Li, S. Zhang, L. Fang, Q. Jiang, and F. Zhao, "Autoalignv2: Deformable feature aggregation for dynamic multi-modal 3d object detection," in *ECCV*, 2022.
- [45] H. Wang, H. Tang, S. Shi, A. Li, Z. Li, B. Schiele, and L. Wang, "Unitr: A unified and efficient multi-modal transformer for bird's-eye-view representation," in *ICCV*, 2023.
- [46] Y. Xie, C. Xu, M.-J. Rakotosoaona, P. Rim, F. Tombari, K. Keutzer, M. Tomizuka, and W. Zhan, "Sparsefusion: Fusing multi-modal sparse representations for multi-sensor 3d object detection," in *ICCV*, 2023.
- [47] J. Yan, Y. Liu, J. Sun, F. Jia, S. Li, T. Wang, and X. Zhang, "Cross modal transformer: Towards fast and robust 3d object detection," in *ICCV*, 2023.
- [48] M. Contributors, "MMDetection3D: OpenMMLab next-generation platform for general 3D object detection," <https://github.com/open-mmlab/mmdetection3d>, 2020.
- [49] B. Zhu, Z.-T. Jiang, X. Zhou, Z. Li, and G. Yu, "Class-balanced grouping and sampling for point cloud 3d object detection," *Cornell University - arXiv, Cornell University - arXiv*, Aug 2019.
- [50] I. Loshchilov and F. Hutter, "Decoupled weight decay regularization," *Learning, Learning*, Nov 2017.
- [51] L. N. Smith, "Cyclical learning rates for training neural networks," in *2017 IEEE Winter Conference on Applications of Computer Vision (WACV)*, Mar 2017.

- [52] K. He, X. Zhang, S. Ren, and J. Sun, "Deep residual learning for image recognition," in *2016 IEEE Conference on Computer Vision and Pattern Recognition (CVPR)*, Jun 2016.